Large and Rapid Temperature Reduction of Organic Solutions with Subcritical CO_2

Sameer V. Dalvi and Mamata Mukhopadhyay
Dept of Chemical Engineering, IIT Bombay, Mumbai 400076, India

DOI 10.1002/aic.11302
Published online September 26, 2007 in Wiley InterScience (www.interscience.wiley.com).

The production of ultra-fine solid particles with narrow size distribution requires creation of a very large, rapid, and uniform supersaturation in the solution of the solid substance. This is facilitated by a rapid, uniform, and large reduction of the solid solubility in the solution and can be achieved either by drastically reducing the temperature of solution or by drastically increasing the CO_2 solubility for achieving the antisolvent effect. As these processes have some disadvantages, a simple technique is reported in this work for imparting the large, uniform, and rapid reduction of temperature in the solution for the required supersaturation. This entails pressure reduction over the gas-expanded liquids utilizing subcritical CO_2 at a relatively low pressure in the range of 40–70 bar and near ambient temperature of 303 K for creating a temperature drop of 30–70 K in the solution within seconds. The present article enunciates the principle of this new technique and analyses the effects of various process parameters on the reduction of temperature of the CO_2-expanded organic solutions. © 2007 American Institute of Chemical Engineers *AIChE J,* 53: 2814–2823, 2007
Keywords: gas-expanded liquids, temperature drop, subcritical CO_2, pressure reduction

Introduction

Particle design presently constitutes a major developmental activity, mainly in the areas of pharmaceuticals, cosmetics, specialty chemicals, and catalysts (biochemical).[1–41] Often these products are required in the form of nanoparticles, microparticles, microfibers, or microcapsules with narrow particle size distribution (PSD). Production of such nanoparticles/microparticles requires creation of a very rapid, uniform, and extremely high supersaturation in the solution.[23] Conventionally milling, grinding, spray drying, and crystallization from solution are some processes used to produce these particles. Out of these, the most common is thermal or antisolvent crystallization of a solid from its solution in an organic solvent and involves reduction of solubility of the solid in the solution to build up the required supersaturation. In conventional thermal crystallization, the supersaturation built-up in the solution is low, nonuniform, and slow, yielding poor control of particle size and resulting in wide PSD, in addition to several other disadvantages.[23] In recent years, supercritical (SC) or subcritical CO_2 has been utilized as solvent, cosolvent, or antisolvent in several processes for the production of ultra-fine solid particles with narrow PSD.

Several processes have been developed using SC CO_2 for the production of nanoparticles. The method of depressurization crystallization uses SC CO_2 as a solvent for rapid expansion of the SC solution (RESS)[1–16] or for precipitation from gas-saturated solution (PGSS)[1,16–22] for reducing the equilibrium solid solubility in the SC or liquid solution, respectively. On the other hand, the antisolvent crystallization processes [e.g., gas antisolvent crystallization, supercritical antisolvent crystallization (SAS), precipitation from compressed antisolvent, supercritical enhanced dispersion of solutions, and aerosol solvent extraction of supercritical solutions][1,23–36] use SC CO_2 as an antisolvent (which is highly soluble in an organic solvent) for reduction of the equilibrium solid solubility in the solution. The SAS process is very rapid because of the two-way diffusion of solvent and antisolvent CO_2 from and to the atomized

Correspondence concerning this article should be addressed to S. V. Dalvi at sameervd@iitb.ac.in.

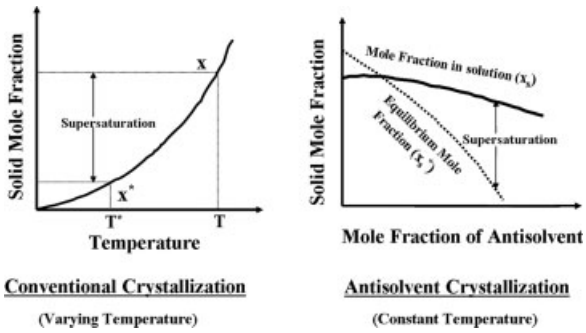

Figure 1. Comparison of conventional crystallization and antisolvent crystallization.

droplet, respectively.[36] In the depressurization of expanded-liquid organic solutions (DELOS)[37–40] and PGSS processes, a temperature drop in the solution is achieved by the Joule–Thompson expansion. In these processes, the solution of a solid in an organic solvent or the melt of a solid to be crystallized is saturated with SC CO_2 before expansion through a nozzle. As the J–T expansion is a steady-state process on a continuous flow mode where the upstream pressure and temperature are kept constant, a low temperature is obtained in the downstream flow at subcritical or ambient pressure. Thus, the reduction in temperature in the DELOS process or the increase in CO_2 mole fraction in the SAS process reduces the equilibrium solid solubility in the solution to create the required supersaturation, as shown in Figure 1. However, these SC CO_2 processes suffer from several drawbacks, such as requirements of (i) very high pressures in the order of 200–400 bar for achieving high solubility of solid solute in SC CO_2 (as in the case of RESS or PGSS), as many solids have poor solubility at lower (less than 200 bar) pressures; (ii) high pressure CO_2 pumps for attaining pressures as high as 120–400 bar; (iii) specially designed nozzle devices of micrometer size (of the range 50–70 μm) for spraying the solution, which is prone to clogging; (iv) accurate control of pressure, temperature, flow rates, and mole fraction; and (v) usage of a large amount of SC CO_2. Accordingly, the objective of this work has been to evolve a process for attaining the large, rapid, and uniform supersaturation, while overcoming the above requirements, i.e., avoiding the usage of any specially designed nozzle and high-pressure pumps. The process is aimed at creating a large and rapid temperature drop in the solution by employing rapid pressure reduction in the vapor space (which is essentially pure CO_2) over the CO_2-expanded liquid solution of the solid solute.[42]

The Process Principle

The process is based on the fact that CO_2 generally has high solubility in organic solvents. When subcritical CO_2 is dissolved in an organic solvent at an initial pressure (less than its vapor pressure) at ambient temperature, the volume of solution expands with a rise in temperature because of the heat of dissolution. To retain the near ambient temperature steady in the solution, the solution is stirred and cooled for removing the heat of dissolution. The space above the solution essentially contains CO_2, as the solvent has a very low vapor pressure at the prevailing temperature. The pressure over the solution is reduced to ambient pressure by allowing CO_2 to escape through the valve, while vigorous CO_2 liberation takes place from the solution. This process of liberation of dissolved CO_2 from the solution requires heat, which is absorbed from the solution itself, thereby causing a reduction in the solution temperature. This simultaneous heat and mass transfer continues till the cessation of liberation of CO_2 from the solution. The solubility of CO_2 in the solution is negligible at atmospheric pressure.[43,44] The vigorous liberation of CO_2 from the solution enables uniform mixing resulting uniform temperature in the solution. The larger the liberation of dissolved CO_2, the larger is the heat of vaporization required to be absorbed from the solution. This implies that a drastic and almost instantaneous reduction in temperature of the solution can be achieved with vigorous ebullition of CO_2 on rapid reduction of pressure. Thus, the process of large, uniform, and instantaneous reduction of temperature in the solution, essentially involves two steps, namely (i) dissolution of CO_2 in the organic solvent at subcritical pressures and near ambient temperature and (ii) the reduction of pressure over the CO_2-expanded organic solvent.

Experimental

Apparatus and experimental procedures

Figure 2 shows the experimental set-up used for the production of low temperatures using CO_2-expanded liquids. The set-up consists of a stainless-steel high-pressure vessel with an internal volume of 1.09 l with an L:D ratio of 2.5 (supplied by M/S Sharad Engineers Pvt., Mumbai, India). The vessel is made of SS316 and can be operated up to 300 bar and 373 K. A pressure indicator having a range from 0 to 480 bar and an accuracy of $\pm$0.1 bar is used for measuring the pressure. The temperature is measured using a resistance temperature detector with an accuracy of $\pm$0.1 K. A rupture disc is also provided on the vessel for safety. The vessel is connected to a CO_2 cylinder from which CO_2 is directly loaded into the vessel through an inlet valve (V_1) and a dip tube. The dip tube having an internal diameter of 0.3 cm and an external diameter of 1 cm is provided to ensure the bubbling of CO_2 in the solution for easy and fast dissolution of CO_2 in the solvent/solution charged in the vessel. The vessel is provided with an outlet valve (V_2) on the top of the vessel for rapid reduction of pressure.

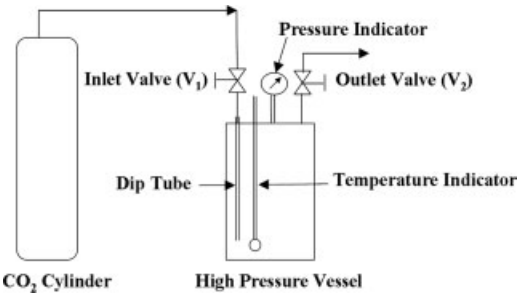

Figure 2. Schematics of experimental set-up for the process.

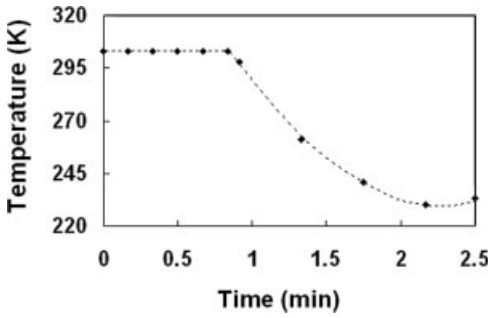

Figure 3. Temperature kinetics of CO_2-expanded acetone by pressure reduction from the initial pressure of 68 bar, temperature of 303 K, and solvent volume of 100 ml.

The high-pressure vessel with and without an organic solvent is first loaded with subcritical CO_2 at 30–70 bar. The temperature is then stabilized to an initial temperature of T^i by cooling and stirring the contents of the vessel, as its temperature rises by the heat liberated due to dissolution of CO_2. The pressure in the autoclave is reduced to atmospheric pressure P^o from the initial pressure P^i within a time span of 0.5–2 min and the temperature of the solution starts decreasing instantaneously. A temperature indicator continuously records the change in the solution temperature till the vessel is completely depressurized as illustrated in Figure 3 for the CO_2-expanded acetone solution.

Materials

CO_2 having purity of 99.99% (Sicgil Industrial Gases, India) was used for the experiments. Different organic solvents used are acetone (99.5% pure from Sd-fine Chemicals, India), ethanol (99.9% pure from Hayman, UK), dimethyl sulfoxide (99.0% pure from Qualigens Fine Chemicals, India), toluene (99.5% pure, Merck, India), carbon tetrachloride (99.5% pure, Merck), and ethyl acetate (99.0% pure, Qualigens Fine Chemicals). These were used without further purification.

Results and Discussions

Temperature drop of pure CO_2 by pressure reduction

The behavior of temperature drop of pure CO_2 by depressurization has been first ascertained, in view of the fact that organic solvents can have very high solubility of CO_2. For example, its mole fraction in the CO_2-expanded solutions could be in the range of 0.96–0.98. Figure 4 shows the behavior of the effect of initial pressure on the experimentally observed temperature drops of pure CO_2 by depressurization from an initial pressure in the range of 30–75 bar and 303 K. The reduction of pressure in the vessel completely filled with liquid CO_2 makes the vessel content gush out with vigor. It can be seen that the slope of temperature drop with pressure drop is very high (12 K/bar) when the initial pressure is in the range of 72–75 bar, whereas it is quite low (0.16 K/bar) in the initial pressure range of 70–30 bar. CO_2 has a vapor pressure of 72.1 bar at 303 K. Thus, at pressures above 72.1 bar and at 303 K, CO_2 is in the liquid phase and the reduction in its pressure causes vaporization of CO_2 and absorption of latent heat of vaporization from the liquid phase itself. Accordingly, depressurization from an initial pressure above 72.1 bar induces temperature drops as large as 70 K. On the other hand, CO_2 exists in gaseous phase for any pressure below 72.1 bar and at 303 K. Thus, depressurization from such an initial pressure does not induce large temperature drops, as there is no phase-change taking place and it is only the thermodynamic work of displacement that is responsible for the temperature drop in the case of gaseous CO_2. The thermodynamic work needed to force the CO_2 out from the vessel causes the internal energy of the contents to decrease, and hence the temperature of the gas remaining in the vessel decreases. The phenomenon of creating a large temperature drop by depressurization of pure liquid CO_2 has been extended to the gas-expanded liquids for the production of low temperatures, as many organic solids are quite soluble in organic solvents and this phenomenon can be utilized to precipitate fine particles from solution.

Temperature drop of CO_2-expanded solvents by pressure reduction

The temperature drop in the gas (CO_2)-expanded liquids is due to liberation of CO_2, which in turn depends on the initial CO_2 dissolution in the solution. Thus, the dependence of the temperature drops observed for various CO_2-expanded solvents has been analyzed on the process parameters, such as initial pressure (20–75 bar), initial temperature (277–318 K), initial volume fraction of the solvent in the vessel, and nature of the solvent, as outlined in the following subsections.

Effect of Initial Pressure. Figure 4 shows the effect of initial pressure on temperature drops observed in the CO_2-expanded acetone by reduction of pressure. At low pressures (1–5 bar), the temperature drop is almost zero, because at such low pressures CO_2 solubility in the solution is negligible. But an increase in pressure increases the temperature drop observed after depressurization, as an increase in initial pressure facilitates more dissolution of CO_2 in the solution. It can be seen that at higher initial pressures in the range of 67–75 bar, the temperature drops of the CO_2-expanded liquid almost

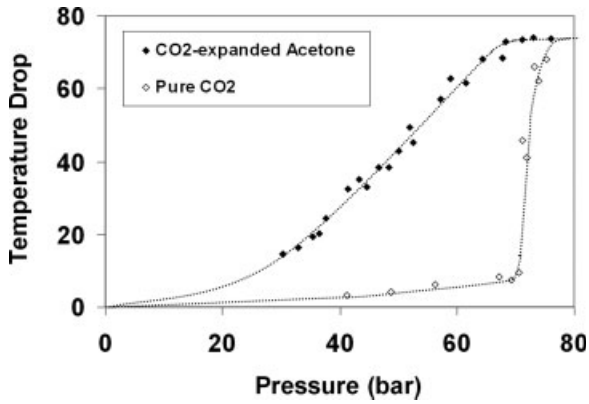

Figure 4. Effect of initial pressure on temperature drops of pure CO_2 and CO_2-expanded acetone (v_{2i} = 100 ml) by pressure reduction from initial temperature 303 K.

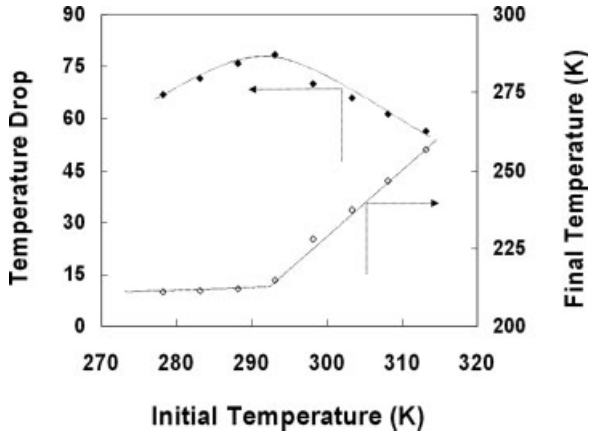

Figure 5. Effect of initial temperature on temperature drop and final temperature of CO_2-expanded ethyl acetate, by pressure reduction from P_i of 72.6 bar for v_{2i} = 100 ml.

match with those of pure liquid CO_2. At high initial pressures, the mixtures contain mostly CO_2 (with CO_2 mole fraction in the range of 0.96–0.98) and hence the temperature drops of such mixture match with those observed with pure liquid CO_2.

Dissolution of CO_2 in an organic solvent causes volume expansion of solvent with an increase in the liquid level in the vessel. At and above a certain pressure, the vessel is completely filled and hence no more dissolution of CO_2 is possible. Therefore, a further increase in pressure above this filling pressure, P^*, does not allow more CO_2 to be dissolved and thus the CO_2 dissolution remains constant. As a result, there is no further increase in temperature drop obtainable from such a solution, even if its pressure is increased after the vessel is completely filled. Thus, when the initial pressure is increased to 67 bar or above, the temperature drop observed remains almost constant as can be seen from Figure 4.

Effect of Initial Temperature. Figure 5 shows the effect of initial temperature on the temperature drops of the CO_2-expanded ethyl acetate solution by depressurization from an initial pressure of 72.6 bar. It is observed that the lower the initial temperature T^i, the higher are the temperature drops observed up to T^i of 293.2 K. At $T^i < 293.2$ K, the temperature drop starts decreasing with decrease in T^i. There are two factors responsible for this namely (i) the final temperature T^o obtained after depressurization from $T^i < 293.2$ K, remains invariant with the initial temperature. This is due to the reason that the vessel is completely filled and hence there is no increase in CO_2 dissolution with a decrease in temperature. And (ii) the other factor is the heat in-leak from the surroundings to the vessel. It may be noted that the vessel is not insulated due to the possible requirement of initial cooling for dissipating the heat of CO_2 dissolution. As depressurization proceeds, the heat for liberating CO_2 is taken from the solution and at the same time the heat is also leaked into the solution from the vessel and surroundings because of a large temperature gradient. Figure 6 shows the time required for depressurization of CO_2-expanded ethyl acetate for different initial temperatures, T^i. The lower the initial temperature T^i, the higher is the time required for depressurization. The increase in depressurization time can be attributed to the increase in the amount of CO_2 dissolved in solvent with decrease in initial temperature T^i. If depressurization time increases because of release of large amount of CO_2, then the heat in leak from the vessel also increases. Thus, the heat in leak and constancy of CO_2 dissolution due to completely filled vessel condition are the two factors responsible for the decrease in the temperature drops observed if the initial temperature is <293.2 K.

Effect of Initial Volume Fraction of Solvent in the Vessel. Figure 7 shows the effect of initial volume percent of solvent in the vessel on the temperature drop. The temperature drop of CO_2-expanded ethyl acetate after depressurization from P^i of 72.6 bar and T^i of 303 K decreases with an increase in the initial volume percent of solvent in the vessel. As the initial volume of solvent (v_2^i) charged in the vessel increases the mole fraction of CO_2 at which the vessel gets completely filled with CO_2-expanded solvent decreases. Also the volume percent spillage, defined as the volume percent of solvent lost during depressurization, increases with an increase in the initial volume percent of solvent in the vessel (as shown in Figure 7). Both these factors, namely (i) the

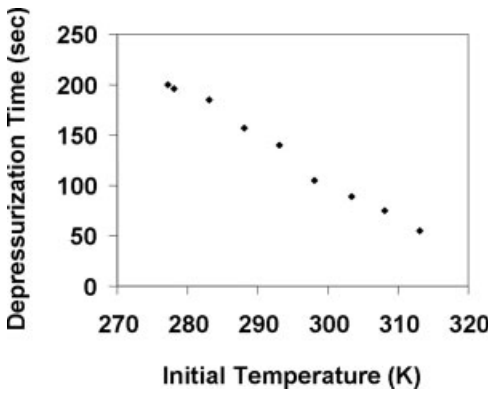

Figure 6. Effect of initial temperature on time of depressurization from P_i = 72.6 bar and v_{2i} = 100 ml.

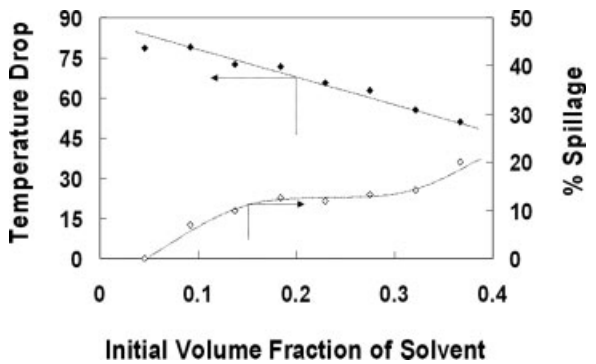

Figure 7. Effect of initial volume fraction of solvent in the vessel on temperature drop and % spillage of CO_2-expanded ethyl acetate by depressurization from P_i = 72.6 bar at T_i = 303 K.

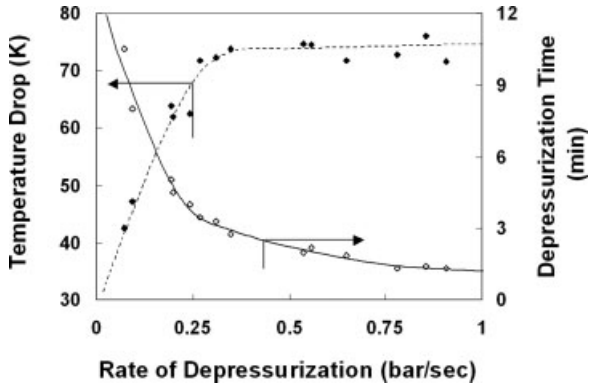

Figure 8. Effect of depressurization rate on the temperature drop of CO_2-expanded ethyl acetate from P_i = 72.6 bar, T_i = 303 K and v_{2i} = 100 ml in a 1.09-l high-pressure vessel.

loss of solvent with CO_2 during depressurization and (ii) constancy of CO_2 dissolution after the vessel is completely filled, cause the temperature drop to decrease with an increase in the initial volume percent of solvent in the vessel.

Effect of Depressurization Rate. Figure 8 shows the effect of depressurization rate on the temperature drop of CO_2-expanded ethyl acetate obtained by depressurization from 72.6 bar and 303 K and time for depressurization (t_{DP})for 100 ml of the solvent in a 1.09-l high-pressure vessel. It can be seen that the temperature drop increases with an increase in depressurization rate, at depressurization rate less than 0.3 bar/s. However, at depressurization rate above 0.3 bar/s, the temperature drop obtained is almost constant (or rate of increase in temperature with depressurization rate is very low) as the depressurization rate increases further. As mentioned earlier, the temperature drop mainly depends on liberation of moles of CO_2 and external heat in-leak from the surroundings. This external heat in-leak directly depends on the time of depressurization, as during this time period, heat leaks in. Initially, when the depressurization rate is low, the time for complete depressurization is very high (Figure 8) and hence large amount of heat leaks in and temperature drop obtained is low. As the depressurization rate increases the time required for the depressurization decreases and hence heat in-leak in the solution also decreases. This causes the temperature drop to increase with an increase in depressurization rate. However, at higher depressurization rates time for depressurization becomes almost constant and hence the temperature drop obtained also remains constant.

Nature of Solvent. It can be seen from Figure 9 that the temperature drops of CO_2-expanded solvents by depressurization are always higher than that by the depressurization of pure CO_2. This confirms that the reduction of pressure over the solution causes CO_2 liberation from the solution, which in turn absorbs heat from the solution and instantaneously lowers the temperature. It can also be seen that the temperature drop of CO_2-expanded acetone by pressure reduction is the highest and that produced by CO_2-expanded ethanol is the lowest among all the CO_2-expanded liquids. This may be attributed to the solubility of CO_2 in different solvents. The polarity of the solvents is a crucial parameter deciding the solubility, though it depends on many other factors. Acetone is polar-aprotic (PA), a relatively nonpolar solvent when compared with ethanol, which is polar-protic, i.e., highly polar. CO_2 being nonpolar (NP), its solubility in acetone is higher than in ethanol at any pressure, which is why the temperature drop produced by CO_2-expanded acetone is higher than that produced by CO_2-expanded ethanol.

Analysis on the Effect of CO_2 Dissolution on Temperature Drop

The temperature drop of the CO_2-expanded solvent by pressure reduction mainly depends on the amount of CO_2 liberated from the solution after depressurization. The amount of CO_2 liberated from the solution can be estimated from (i) the initial CO_2 solubility x_1^i in the solvent at initial pressure P^i and initial temperature T^i and (ii) the final CO_2 solubility x_{1o} at final pressure P^o and temperature T^o. The system of CO_2–acetone is chosen as the model system to illustrate these calculations. Table 1 presents the temperature drops produced by the pressure reduction of CO_2-expanded acetone from different initial pressures at 303 K when the initial volume fraction of acetone in the vessel is 0.092 (i.e., v_{2i} = 100 ml).

Estimation of initial CO_2 mole fraction, x_1^i

As the vessel contents are equilibrated for sufficient time before depressurization, the initial CO_2 mole fraction x_1^i is assumed to be the equilibrium CO_2 mole fraction in the solution at the prevailing initial pressure and temperature. For ensuring vapor–liquid equilibrium (V-L-E) in the vessel, it is necessary to have some vapor space above the solution. However, the dissolution of CO_2 in an organic solvent causes volume expansion of the solvents[45] and will fill the vessel completely at a certain filling pressure P^* and a maximum of CO_2 mole fraction. In such a case, the initial CO_2 mole fraction x_1^i in the solution can be calculated based on the maximum allowable expanded volume of the CO_2-expanded sol-

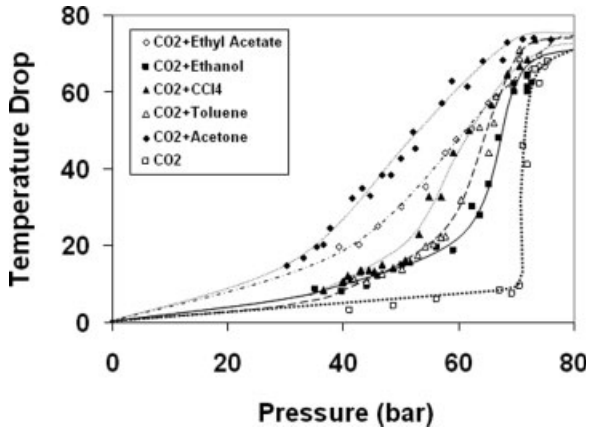

Figure 9. Effect of initial pressure on temperature drop in different CO_2-expanded solvents by depressurization from T_i = 303 K for v_{2i} = 100 ml.

Table 1. Temperature Drops Obtained for CO_2(1)–Acetone(2) System

P_i, bar	T_i, °C	T_o, °C	ΔT, K
70.41	29.6	−44.0	73.6
68.37	30.3	−42.9	72.9
67.69	30.3	−38.0	68.3
65.65	30.0	−32.7	62.7
64.29	30.0	−32.6	62.6
61.56	30.3	−31.2	61.5
58.84	30.1	−32.7	62.7
57.14	30.0	−27.2	57.2
52.04	30.0	−19.5	49.5
50.07	30.3	−12.5	42.8
48.30	30.1	−8.3	38.4
46.67	30.5	−8.0	38.5
44.69	30.1	−2.8	32.9
43.33	30.3	−4.8	35.1
41.50	29.8	−2.6	32.4
37.62	30.3	5.9	24.4
36.53	30.1	10.0	20.1
35.31	30.2	10.8	19.4
33.00	29.5	13.0	16.5
30.27	30.0	15.2	14.5

vent (equaling the working volume of the vessel) as explained in Figure 10. Thus, the following procedure is used to calculate the initial CO_2 mole fraction x_{1i} in the solution.

1. At a given initial pressure and temperature, the molar volume[46] of the CO_2-expanded solvent and the total volume are calculated from the number of moles of solvent initially charged in the vessel at different CO_2 mole fractions.
2. The mole fraction of CO_2 in the solution at which the vessel is completely filled (i.e., for the condition when the total volume = the working volume of the vessel) is calculated and denoted as mole fraction as x_1^v (as explained in Figure 11).
3. If the initial pressure is less than the mixture critical pressure of the binary CO_2-solvent system at the prevailing temperature then the equilibrium liquid phase CO_2 mole fraction x_1^e (as explained in Figure 12) at the prevailing pressure and temperature condition is calculated as follows:
   A. If $x_1^v < x_1^e$, then the vessel is completely filled and V-L-E cannot exist in the vessel. Therefore, x_{1v} is the mole fraction of CO_2 in the expanded-solvent x_{1i} at the initial condition.
   B. If $x_1^v > x_1^e$, then the vessel is not completely filled, which allows V-L-E to exist and, therefore, x_1^e is the initial CO_2 mole fraction x_1^i in the expanded solvent.
4. If the initial pressure is greater than the vapor pressure of CO_2 or the mixture critical pressure of the binary CO_2-solvent system at the prevailing temperature then the initial CO_2 mole fraction can only be determined from expanded volume, because at this pressure the two-phase vapor–liquid region does not exist and the binary mixture (CO_2-expanded solvent) either exists as a compressed liquid or SC fluid depending on the CO_2 mole fraction in the mixture. Therefore, x_{1v} is the initial mole fraction x_1^i of CO_2 in the expanded-solvent at the initial condition.

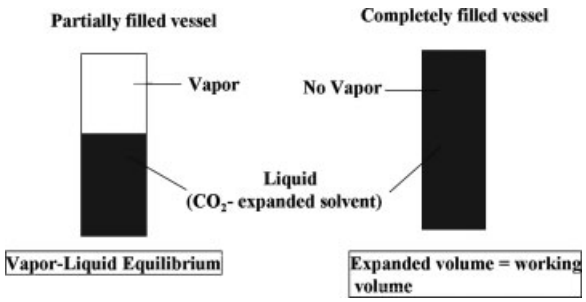

Figure 10. Conditions prevailing in a high-pressure vessel containing CO_2-expanded solvent before pressure reduction.

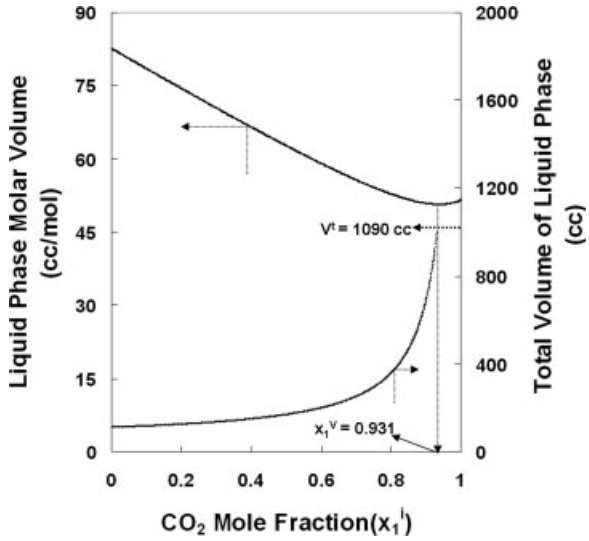

Figure 11. Effect of initial mole fraction x_{1i} on molar volume and the maximum expanded volume for CO_2-expanded acetone at P_i = 70 bar, T_i = 298 K, and v_{2i} = 100 ml.

Calculation of final CO_2 mole fraction, x_{1o}

The depressurization may not remove all of the CO_2 from the solution as CO_2 gas has some solubility in the solvent at the final pressure of 1 atm and temperature as low as 223 K (−50°C). Different techniques have been examined[43] to predict gas–liquid equilibrium (G-L-E) at pressures less than

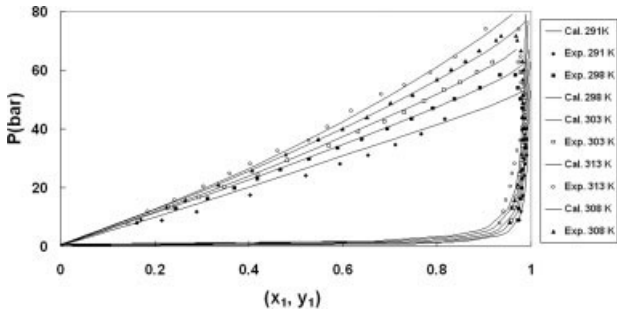

Figure 12. Comparison of predicted isothermal vapor–liquid equilibrium data for binary CO_2(1)–acetone(2) system with experimental data.[49]

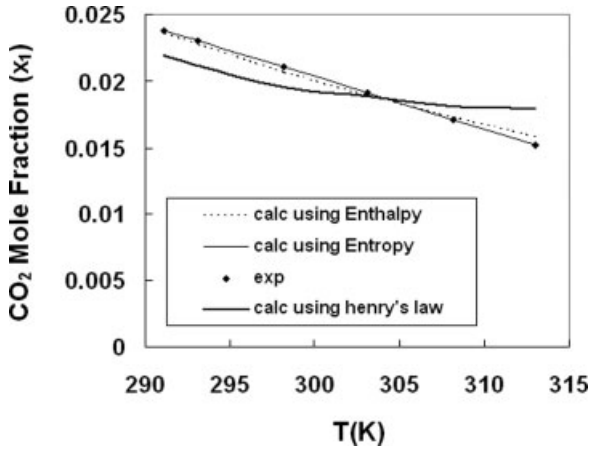

Figure 13. Comparison of predicted gas–liquid equilibrium (G-L-E) data for CO_2(1)–acetone(2) at 1 atm.

5 atm and temperatures as low as 223 K (−50°C). Figure 13 compares the solubility predictions based on the Henry's law at a pressure of 1 atm with the experimental data, which deviate at high as well as low temperatures. The G-L-E data have also been predicted from the enthalpy and entropy of dissolution by using the experimental data.[44] The solubility predicted using the enthalpy and entropy of dissolution matches closely with the experimental data. Also it can be noted that the predictions based on the entropy of dissolution are more accurate when compared with the predictions based on the enthalpy of dissolution. Therefore, the concept of the entropy of dissolution has been used for G-L-E in this work for the prediction of the final CO_2 mole fraction after the depressurization of the CO_2-expanded solution. It can be seen that the CO_2 solubility is negligible at 1 atm even at low temperatures.

Calculation of CO_2 moles liberated by depressurization

Table 2 presents the initial CO_2 mole fraction x_{1i} calculated based on the expanded volume or V-L-E calculations and the final CO_2 mole fraction x_{1o} based on G-L-E calculations. The number of moles of CO_2 evaporated is then calculated by using x_1^i, x_1^o and the initial moles of acetone charged in the vessel. Figure 14 shows the dependence of the temperature drop experimentally observed on the number of moles of CO_2 liberated from the solution. It can be seen that the temperature drop in the solution increases with an increase in the number of moles of CO_2 liberated from the solution. Thus, it is validated that the temperature drop of the CO_2-expanded solvent by pressure reduction depends directly on the number of moles of CO_2 liberated from the solution. Initially, the rate of change of temperature with the change in number of moles of CO_2 liberated is quite sharp but it flattens as the number of moles of CO_2 liberated from the solution increases. As the temperature drop increases due to more number of moles of CO_2 liberated from the solution, the temperature gradient available for the heat transfer from the surroundings to the vessel wall increases and hence the rate of change of temperature drop with CO_2 moles liberated decreases and the curve flattens out. However, this flat portion of the curve is again followed by a stiff vertical curve where the temperature of solution changes drastically even though the number of CO_2 molecules liberated from the solution remains constant. For the range of 30 bar to P^* (the filling pressure), the CO_2-expanded liquid exists in two-phase region. The pressure reduction over the CO_2-expanded liquid from this range of initial pressure liberates only CO_2 from the solution. At initial pressures above P^*, the CO_2-expanded liquids enter into a compressed liquid (single phase) region and the vessel is completely filled under such conditions. The pressure reduction of CO_2-expanded liquids from such an initial pressure (above P^*) causes immediate flashing and spillage of the liquid. Spillage causes the loss of the solvent as well as large amount of CO_2 (as CO_2 mole fraction in the liquid phase can be as high as 0.92–0.95 at pressure higher than P^*). After flashing, only CO_2 is liberated from the solution due to pressure reduction. Thus, for initial pressures above P^*, the temperature of the solution decreases because of both the expansion of single phase (flashing) as well as

Table 2. Temperature Drop in CO_2(1)–Acetone(2) System Produced by Pressure Reduction from 303 K with V_2 = 100 ml in 1.09 l High-Pressure Vessel

P_i, bar	x_{1V} by Max. Vol.	x_{1e} by V-L-E	x_{1i}	N_{1i}, mol	x_{1o}	N_{1o}, mol	ΔT, K
70.41	0.934	0.977	0.934	19.298	0.090	0.135	73.6
68.37	0.934	0.959	0.934	19.298	0.087	0.130	72.9
67.69	0.934	0.953	0.934	19.298	0.078	0.116	68.3
64.29	0.934	0.920	0.920	19.298	0.068	0.101	62.6
61.56	0.934	0.893	0.893	15.709	0.067	0.100	61.5
58.84	0.934	0.865	0.865	11.363	0.068	0.097	62.7
57.14	0.934	0.846	0.846	8.711	0.061	0.100	57.2
52.04	0.934	0.789	0.789	7.519	0.051	0.088	49.5
50.07	0.934	0.767	0.767	5.117	0.044	0.074	42.8
48.3	0.934	0.746	0.746	4.479	0.040	0.063	38.4
46.67	0.934	0.726	0.726	3.995	0.040	0.057	38.5
44.69	0.934	0.701	0.701	3.608	0.036	0.057	32.9
43.33	0.934	0.684	0.684	3.199	0.037	0.051	35.1
41.5	0.934	0.660	0.660	2.952	0.036	0.053	32.4
37.62	0.934	0.609	0.609	2.124	0.030	0.042	24.4
36.53	0.934	0.594	0.594	1.996	0.028	0.039	20.1
35.31	0.934	0.577	0.577	1.863	0.027	0.038	19.4
33.0	0.934	0.545	0.545	1.633	0.027	0.037	16.5
30.27	0.934	0.506	0.506	1.395	0.025	0.035	14.5

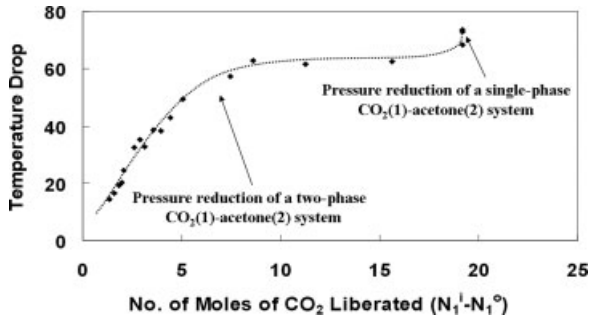

Figure 14. Dependence of temperature drop on the number of moles of CO_2 liberated, for CO_2–acetone system at 303 K.

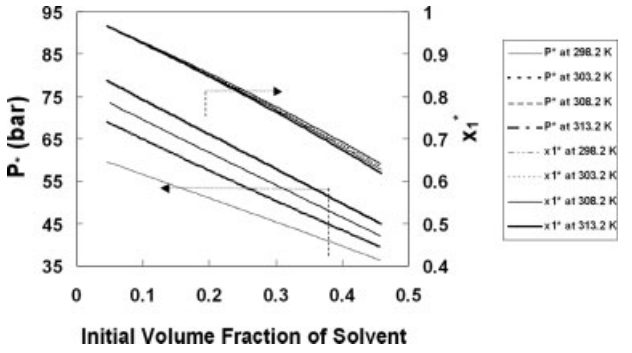

Figure 16. Effect of initial volume fraction of solvent on P^* and x_1^* at different T_i for CO_2-expanded acetone.

the liberation of CO_2 from liquid in the two-phase region. Moreover, an increase in initial pressure above P^* increases the pressure drop required to bring a liquid again in two-phase region. Hence, the latent heat of vaporization of a mixture taken from the solution during flashing also increases. Therefore, the drastic increase in temperature drop is observed even though the number of CO_2 moles dissolved in the solution remains constant.

*Estimation of filling pressure, P**

The filling pressure P^* is defined as the CO_2 pressure at which the vessel with an initial volume fraction of solvent gets completely filled due to dissolution of CO_2 at the initial temperature. Thus, P^* is the limiting pressure at which the binary two-phase system of CO_2-solvent enters into a single-phase from a two-phase region. The corresponding CO_2 mole fraction in the solution x_1^* is the highest CO_2 solubility. Figure 15 schematically shows the procedure to calculate the filling pressure P^* and the corresponding CO_2 solubility x_1^* for CO_2-expanded ethyl acetate at $T_i = 303$ K and $v_{2i} = 100$ ml. P^* is obtained from the intersection of x_1^v (calculated based on volume expansion) and x_1^e (calculated based on V-L-E). At a constant initial temperature T^i, P^* and x_1^* depend on the initial volume fraction of the solvent in the vessel.

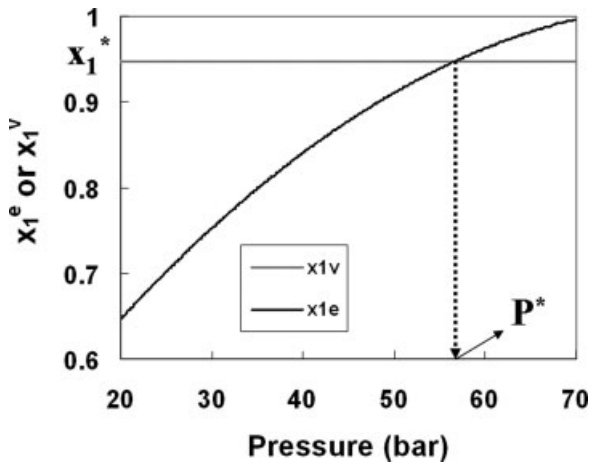

Figure 15. Determination of P^* and x_1^* for CO_2-expanded ethyl acetate for $v_{2i} = 100$ ml and $T_i = 303.2$ K.

Figure 16 shows the effect of the initial volume fraction of solvent on P^* and x_1^* at various initial temperatures for CO_2–acetone system. It can be seen that at any initial temperature, T^i, P^* decreases with an increase in the initial volume fraction of solvent as the vessel gets filled at lower pressures with a higher volume of solvent charged initially. Similarly, P^* is lower at a lower temperature as CO_2 solubility in an organic solvent increases with a decrease in temperature and vessel gets filled completely at lower pressures. However, x_1^* does not vary much with the change in initial temperature though it decreases with an increase in the initial volume fraction. This is due to the reason that the vessel gets completely filled at lower CO_2 mole fraction for a higher initial volume of solvent charged in the vessel.

It is to be noted that P^* is the limiting pressure at which vessel should be charged with CO_2 at a particular value of the initial volume fraction of solvent and T^i as an increase in pressure above this value does not further change CO_2 solubility in the CO_2-expanded solvent significantly. Also, x_1^* is the maximum CO_2 solubility in the CO_2-expanded solvent at any T^i and initial volume fraction of the solvent. Thus, x_1^* is the solubility of CO_2 that should be attained in the CO_2-expanded solvent to attain the highest possible temperature drop. x_1^* does not change significantly with the change in initial temperature T^i as it practically remains constant (Figure 15). This implies that there is no need for an accurate control of initial temperature of the solution to obtain the highest possible temperature drop.

Conclusions

A very large and uniform temperature reduction of an organic solvent to as low as -70°C can be achieved within a very short span of time (as low as 0.5 min) by dissolving subcritical carbon dioxide, followed by pressure reduction from 30 to 70 bar. The mechanism for such a drastic temperature reduction has been ascertained and illustrated for CO_2-expanded acetone as the model system. The temperature drop observed after the pressure reduction depends on the number of moles of CO_2 liberated from the solution and hence on the number of moles of CO_2 dissolved in the solu-

tion initially. The larger is the number of moles of dissolved CO_2, the higher will be the temperature drop. Thus, a solvent having a high CO_2 solubility should be selected in the process. The solvent should be preferably NP or PA, as the CO_2 solubility in such a solvent is higher than in the polar solvents such as ethanol. Also, the working volume of the vessel should be designed in such a way that the vessel is charged with the required initial volume fraction of solvent, and is pressurized up to the corresponding filling pressure for attaining the maximum CO_2 dissolution and thus the process ensures highest temperature drops. The highest CO_2 dissolution and the filling pressure strongly depend on the volume fraction of solvent in the vessel and do not much depend on the initial temperature. Utilizing this concept of the temperature reduction by pressure reduction over CO_2-expanded liquids, a new process for production of ultra-fine particles, namely, "Precipitation by Pressure Reduction of Gas-expanded Liquids (PPRGEL)" has been developed[47,48] and patented.[42]

Notation

C = concentration (mol/cc)
N = number of moles (mol)
P = pressure (bar)
T = temperature (K)
V_t = total volume of liquid phase (cc)
v = liquid molar volume (cc/mol)
x = liquid phase mole fraction
y = vapor phase mole fraction

Subscripts

e = equilibrium condition
i = initial condition
v = related to volume expansion
s = related to solid phase
o = final condition
1 = related to CO_2
2 = related to solvent

Symbols

ρ = change in a variable
* = maximum value of variable, equilibrium value

Literature Cited

1. Jung J, Perrut M. Particle design using supercritical fluids: literature and patent survey. *J Supercrit Fluids*. 2001;20:179–219.
2. Diefenbacher A, Turk M. Phase equilibria of organic solid solutes and supercritical fluids with respect to RESS process. *J Supercrit Fluids*. 2002;22:175–184.
3. Domingo C, Berneds E, Rosmalen G. Precipitation of ultrafine organic crystals from the rapid expansion of supercritical solutions over a capillary and frit nozzle. *J Supercrit Fluids*. 1997;10:39–55.
4. Kayark D, Akman U, Hortacsu O. Micronization of ibuprofen by RESS. *J Supercrit Fluids*. 2003;26:17–31.
5. Meziani M, Pathak P, Sun Y. Supercritical fluid processing technique for polymeric particles and fibers. In: *Proceedings of Seventh International Symposium on Supercritical Fluids*, Orlando, FL, 2005.
6. Mohamed R, Halverson D, Debenedetti P, Prudhomme R. Solid formation after the expansion of supercritical mixtures. In: Johnston KP, Penninger JML, editors. *Supercritical Fluid Science and Technology*. ACS Symposium Series 406. Washington DC: ACS Press, 1989:355–378.
7. Pathak P, Meziani M, Desai T, Sun Y. Nanosizing drug particles in supercritical fluid processing. In: *Proceedings of Seventh International Symposium on Supercritical Fluids*, Orlando, FL, 2005.
8. Sun Y, Guduru R, Lin F, Whiteside T. Preparation of nanoscale semiconductors through the rapid expansion of supercritical solution (RESS) into liquid solution. In: *Proceedings of Seventh International Symposium on Supercritical Fluids*, Orlando, FL, 2005.
9. Subra P, Berroy P, Sauriana J, Domingo C. Influence of expansion conditions on the characteristics of cholesterol crystals analyzed by statistical design. *J Supercrit Fluids*. 2004;31:313–322.
10. Subra P, Berroy P, Vega A, Domingo C. Process performances and characteristics of powders produced using supercritical CO_2 as solvent and antisolvent. *Powder Technol*. 2004;142:13–22.
11. Thakur R, Gupta R. Formation of phenytoin nanoparticles using rapid expansion of supercritical solution with solid cosolvent (RESS-SC) process. *Int J Pharm*. 2006;308:190–199.
12. Thakur R, Gupta R. Rapid expansion of supercritical solution with solid cosolvent (RESS-SC) process: formation of 2-aminobenzoic acid nanoparticles. *J Supercrit Fluids*. 2006;37:307–305.
13. Turk M, Hils P, Helfgen B, Schaber K, Martin HJ, Whal MA. Micronization of pharmaceutical substances by the rapid expansion of supercritical solutions (RESS): a promising method to improve the bioavailability of poorly soluble pharmaceutical agents. *J Supercrit Fluids*. 2000;22:75–84.
14. Turk M. Influence of thermodynamic behaviour and solute properties on homogeneous nucleation in supercritical solutions. *J Supercrit Fluids*. 2000;18:169–184.
15. Turk M. Formation of small organic particles by RESS: experimental and theoretical investigations. *J Supercrit Fluids*. 1999;15:79–89.
16. Palakodaty S, York P. Phase behavioral effects on particle formation processes using supercritical fluids. *Pharm Res*. 1999;16:976–985.
17. Elvassore N, Flabani M, Vezzu K, Bertucco A, Caliceti P, Semenzato A, Salmaso S. Lipid system micronization for pharmaceutical applications by PGSS technique. In: *Proceedings of Sixth International Symposium on Supercritical Fluids*. Versailles, France. 2003;3:1853–1858.
18. Gomes de Azevedo E, Jun L, Veciana J. Modeling of particle formation from a gas-saturated solution process. In: *Proceedings of Sixth International Symposium on Supercritical Fluids*. Versailles, France. 2003;3:1859–1864.
19. Kappler P, Leiner W, Petermann M, Weidner E. Size and morphology of particles generated by spraying polymer-melts with carbon dioxide. In: *Proceedings of Sixth International Symposium on Supercritical Fluids*. Versailles, France. 2003;3:1891–1896.
20. Knez Z. High pressure micronization of polymers. In: *Proceedings of Sixth International Symposium on Supercritical Fluids*. Versailles, France. 2003;3:1870–1865.
21. Rodrigues M, Peirico N, Matos H, Gomes de Azevedo E, Lobato M, Almeida A. Microcomposites theophylline/hydrogenated palm oil from a PGSS process for controlled drug deliver systems. *J Supercrit Fluids*. 2004;29:175–184.
22. Weidner E, Knez Z, Novak Z. PGSS (particles from gas saturated solutions)—a new process for powder generation. In: *Proceedings of Third International Symposium on Supercritical Fluids*. Strasbourg, France. 1994;3:229–234.
23. Reverchon E. Supercritical antisolvent precipitation of micro- and nano-particles. *J Supercrit Fluids*. 1999;15:1–21.
24. Chattopadhyay P, Gupta R. Supercritical CO_2 based production of fullerene nanoparticles. In: *Proceedings of Fifth International Symposium on Supercritical Fluids*, Atlanta, GA, 2000.
25. Dillow A, Denghani F, Foster N. Production of polymeric support materials using a supercritical fluid gas anti-solvent process. In: *Proceedings of Fourth International Symposium on Supercritical Fluids*, Sendai, Japan, 1997.
26. Dixon DJ, Johnston KP, Bodmeier RA. Polymeric materials formed by precipitation with a compressed fluid antisolvent. *AIChE J*. 1993; 39:127–139.
27. Dixon DJ, Luna-Barcenas G, Johnston KP. Microcellular microspheres and microballoons by precipitation with a vapor–liquid compressed fluid antisolvent. *Polymer*. 1994;35:3998–4005.
28. Hong L, Bitemo S, Gao Y, Yuan, Y. Precipitation of microparticulate organic pigments. In: *Proceedings of Fifth International Symposium on Supercritical Fluids*, Atlanta, GA, 2000.
29. Muhrer G, Mazotti M, Muller M. Gas antisolvent recrystallization of an organic compound. Tailoring product PSD and scaling-up. *J Supercrit Fluids*. 2003;29:221–220.

30. Palakodaty S, York P, Hanna M, Pritchard J. Crystallization of lactose using solution enhanced dispersion by supercritical fluids (SEDS) technique. In: *Proceedings of Fifth meeting on Supercritical Fluids*. Kyoto, Japan. 1998;275–280.
31. Rantakyla M. *Particle Production by Supercritical Antisolvent Techniques*, Ph.D. Thesis, Helsinki University of Technology, Helsinki, Finland, 2004.
32. Shekunov B, Hanna M, York P. Particle formation by mixing with supercritical antisolvent at high Reynolds number. *Chem Eng Sci*. 1999;56:2421–2433.
33. Thiering R, Dehghani F, Foster NR. Current issues relating to antisolvent micronisation techniques and their extension to industrial scales. *J Supercrit Fluids*. 2001;21:159–177.
34. Thiering R, Dehghani F, Foster NR. Micronization of model proteins using compressed carbon dioxide. In: *Proceedings of Fifth International Symposium on Supercritical Fluids*, Atlanta, GA, 2000.
35. Wubbolt FE, Bruinsma OSL, de Graauw J, van Rosmalen GM. Continuous gas anti-solvent crystallization of hydroquinone from acetone using carbon dioxide. In: *Proceedings of Fourth International Symposium on Supercritical Fluids*. Sendai, Japan. 1997:63–66.
36. Mukhopadhyay M, Dalvi S. Mass and heat transfer analysis of SAS: effects of thermodynamic states and flow rates on droplet size. *J Supercrit Fluids*. 2004;30:333–348.
37. Munto M, Ventosa N, Veciana J. Crystallization of organic polymers through the DELOS process: influence of the operational parameters on the physicochemical characteristics. In: *Proceedings of Sixth International Symposium on Supercritical Fluids*. Versailles, France. 2003;3:1849–1850.
38. Ventosa N, Sala S, Veciana J. DELOS process: crystallization of pure polymorphic phases from CO_2-expanded solutions. In: *Proceedings of Sixth International Symposium on Supercritical Fluids*. Versailles, France. 2003;3:1673–1676.
39. Ventosa N, Sala S, Veciana J. DELOS process: a crystallization technique using compressed fluids 1. Comparison to GAS crystallization method. *J Supercrit Fluids*. 2003;26:33–45.
40. Ventosa N, Sala S, Veciana J. DELOS process: a crystallization technique using compressed fluids 1. Comparison to GAS crystallization method. *J Supercrit Fluids*. 2003;26:33–45.
41. Tadros M, Adkins C, Russick E, Youngman M. Synthesis of titanium dioxide particles in supercritical CO_2. *J Supercrit Fluids*. 1996;9:172–177.
42. Mukhopadhyay M, Dalvi S. *A Novel Method for Production of Nanoparticles using Subcritical Carbon Dioxide*, Indian Patent No. 544/MUM/2004.
43. Giacobbe FW. Thermodynamic solubility behavior of carbon dioxide in acetone. *Fluid Phase Equilib*. 1992;72:277–297.
44. Dalvi S, Mukhopadhyay M. Prediction of solubility of CO_2 in acetone at low pressures and low temperatures. In press.
45. Badilla J, Peters C, Swaan Arons J. Volume expansion in relation to the gas-antisolvent process. *J Supercrit Fluids*. 2000;17:13–23.
46. Dalvi S, Mukhopadhyay M. Prediction of molar volumes of CO_2 gas-expanded liquids using a new generalized method. *Ind Eng Chem Res*. In press.
47. Dalvi S, Mukhopadhyay M. Precipitation of ultra-fine particles of cholesterol by pressure reduction of gas-expanded liquids (PPRGEL) using sub-critical CO_2. In press.
48. Dalvi S, Mukhopadhyay M, Precipitation of ultra-fine particles of zinc acetate by pressure reduction of gas-expanded liquids (PPRGEL) using sub-critical CO_2. In press.
49. Chang C, Day C, Ko C, Chiu K. Densities and *P–x–y* diagrams for carbon dioxide dissolution in methanol, ethanol and acetone mixtures. *Fluid Phase Equilib*. 1997;131:243–258.

Manuscript received Apr. 20, 2007, and revision received July 31, 2007.